Available online at www.sciencedirect.com
ScienceDirect
Ceramics International 36 (2010) 1063–1067
CERAMICS INTERNATIONAL
www.elsevier.com/locate/ceramint

Electrical properties of Pr_6O_{11}-doped WO_3 capacitor–varistor ceramics

T.G. Wang, G.Q. Shao *, W.J. Zhang, X.B. Li, X.H. Yu

State Key Laboratory of Advanced Technology for Materials Synthesis & Processing, Wuhan University of Technology, Wuhan 430070, China

Received 23 June 2009; received in revised form 22 September 2009; accepted 19 November 2009
Available online 4 January 2010

Abstract

The microstructure and electrical properties of Pr_6O_{11}-doped WO_3 ceramics were investigated. Results showed that the breakdown voltage of doped samples was lower than that of the undoped. The dielectric constant of doped samples was higher than that of the undoped, and the high dielectric constant made Pr_6O_{11}-doped WO_3 ceramics to be applicable as a kind of capacitor–varistor materials. A small content of Pr_6O_{11} could significantly improve nonlinear properties of the samples. The WO_3–0.03 mol% Pr_6O_{11} obtained a large nonlinear coefficient of 3.8, a low breakdown voltage of 8.8 V/mm, and a high dielectric constant of 7.69×10^4 at 1 kHz. The defects theory was introduced to explain the nonlinear electrical behavior of Pr_6O_{11}-doped WO_3 ceramics.

Keywords: C. Electrical properties; Pr_6O_{11}-doped WO_3; Capacitor–varistor; Microstructure

1. Introduction

Varistors are electro-ceramic devices that are widely used to protect electrical and electronic equipments against transient over-voltages. The most important property of a varistor is its nonlinear current–voltage (*I–V*) characteristic, which can be expressed by the equation of $I = KV^{\alpha}$, where K is a constant, α is the nonlinear coefficient. Larger value of α is corresponding to a better varistor. Presently, ZnO-based varistors have been extremely studied and commercially applied in a large variety of power systems and electric circuits [1]. Their typical α values range from 30 to 50 and breakdown voltages exceed 100 V/mm [2], while the latter decides that they aren't in low-voltage application. Some other low-voltage varistors such as TiO_2- and WO_3-based varistors, etc. exhibited larger dielectric constant as well as lower breakdown voltages than ZnO varistors. TiO_2 ceramics [3–4] were reported to possess nonlinear coefficient of 4–7, breakdown voltage below 15 V/mm, barrier voltage of 0.1 V, and dielectric constant of $(4–10) \times 10^4$ at 1 kHz. WO_3 ceramics were reported to have a nonlinear coefficient of 3–7, breakdown voltage of 3–10 V/mm [5] and a high dielectric constant [6]. Moreover, WO_3-based varistors had a smaller nonlinear coefficient, lower barrier voltages (∼0.04 V) [7] and a higher dielectric constant [8] than the TiO_2-based varistors. These imply that WO_3 is a good candidate for a capacitor–varistor with a low breakdown voltage.

The rare-earth oxides such as Pr_6O_{11}, etc. were ever used to amend the nonlinear *I–V* characteristics of ZnO ceramics [9–11]. Recently, Wang et al. [12] found that Tb_4O_7-doped WO_3 ceramics exhibited striking nonlinear electrical properties at high temperature. Yang et al. [6,13] studied the CeO_2-, Dy_2O_3- and La_2O_3-doped WO_3 capacitor–varistor ceramics, in which CeO_2-doped WO_3 had the largest nonlinear coefficient of 6.8. But its breakdown voltage increased to 50.9 V/mm and was not suitable for the low-voltage application. Considering that Pr^{3+} had a larger ionic radius and a smaller valence than the W^{6+}, Pr_6O_{11} dopant as a substantial acceptor could be estimated when doped in a WO_3-based varistor. In this work, the doping effects of Pr_6O_{11} on the microstructure and electrical properties of WO_3 ceramics were investigated.

2. Experimental

Commercially purchased WO_3 (99.0 wt.%) and Pr_6O_{11} (99.99 wt.%) powders were used in this study. The compositions were $(100 - x)$ mol% WO_3 and x mol% Pr_6O_{11}, where $x = 0.01$, 0.03, 0.05 and 0.10, respectively. The mixture of WO_3 and Pr_6O_{11} was milled by agate balls for 12 h in pure ethanol. The milled mixture was dried and then pressed at 40 MPa into

* Corresponding author. Tel.: +86 27 87216912.
E-mail address: gqshao@whut.edu.cn (G.Q. Shao).

0272-8842/$36.00
doi:10.1016/j.ceramint.2009.12.004

pellets of 12 mm in diameter and 2 mm in thickness. The green compacts were air-sintered at 1150 °C for 2 h, and free-cooled to room temperature.

Phases were determined by X-ray diffraction (XRD, Cu Kα, D/MAX-RB, Rigaku Denki, Japan). The microstructure and elements were examined by scanning electron microscope (SEM, JSM-5610LV, JEOL, Japan) combined with energy dispersive X-ray (EDX). The grain sizes were calculated by using Image-Pro Plus 6.0 software. For electrical properties measurement, silver electrodes were fabricated on both sides of samples. The dielectric constant was determined by using an Impedance Analyzer (HP4294A, HP, USA). The current–voltage (*I–V*) characteristics were measured by using a varistor-parametric-tester (CJ1001, Chang Zhou Chuang Jie Lightning Protection Co., Ltd., China) with a stabilized DC power.

The breakdown voltage (E_b, V/mm) was defined as the field density when the current density reaches 1 mA/cm^2. The barrier voltage was determined by Eq. (1) [14]:

$$v_b = E_b d \tag{1}$$

where d (μm) was the grain size. The nonlinear coefficient (α) was obtained from Eq. (2):

$$\alpha = \frac{\log(I_2/I_1)}{\log(V_2/V_1)} \tag{2}$$

where I_2 = 10 mA/cm^2, I_1 = 1.0 mA/cm^2, V_2 and V_1 were the voltages corresponding to the current density of I_2 and I_1, respectively.

The capacitance–voltage (*C–V*) characteristics were measured with an Impedance Analyzer (HP4294A, HP, USA) at 10 kHz. According to the Schottky-barrier model and the obtained *C–V* relation, the donor density (N_d), barrier height (Φ_b), density of interface states (N_t) and the depletion-layer width (t) were determined. N_d and Φ_b were estimated from the slope and the intercept of straight line plots of $(1/C–1/2C_0)^2$ vs. V_{gb} (where C was the capacitance per grain boundary, and V_{gb} was the applied voltage per grain boundary). N_t and t were determined from the following equation and relationship, respectively [15]:

$$N_t = (2\varepsilon N_d \Phi_b/q)^{1/2} \tag{3}$$

$$t = N_t/N_d \tag{4}$$

where ε was the dielectric constant of WO_3, q was the electron charge.

3. Results and discussion

XRD patterns of the pure WO_3 and the doped samples are shown in Fig. 1. Only WO_3 (monoclinic and triclinic) phases are presented, which differ from ZnO-based varistors. SEM micrographs are shown in Fig. 2. The average grain sizes (d, μm) are listed in Table 1. Results showed that the grain size increased while the Pr_6O_{11} content increased, meaning that the dopant could promote grain growth. The largest grain size was corresponding to the WO_3–0.10 mol% Pr_6O_{11} sample.

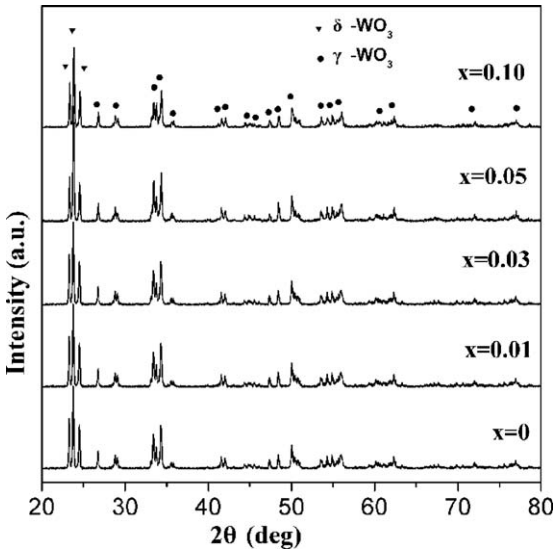

Fig. 1. X-ray diffraction patterns of $(100 - x)$ mol% $WO_3 + x$ mol% Pr_6O_{11} samples.

The microstructure of cross section and corresponding EDX of the WO_3–0.10 mol% Pr_6O_{11} sample showed that only Pr and W elements presented at point A (Fig. 3), which indicated that intergranular phase existed at grain boundary because of the segregation effect of Pr element.

The *I–V* characteristics of different samples are shown in Fig. 4 and Table 1. Results showed that WO_3 doped with 0.03 mol% Pr_6O_{11} had the best nonlinear electrical property since it had the largest nonlinear coefficient of 3.8. The leakage current (I_L) of pure WO_3 sample (0.55 mA) was larger than that of samples doped with 0.01–0.05 mol% Pr_6O_{11}. The minimum I_L value (0.35 mA) was obtained in WO_3–0.03 mol% Pr_6O_{11}. When the Pr_6O_{11} content increased to 0.10 mol%, the I_L value abruptly increased to 0.62 mA. The variation of I_L, on the whole, was opposite to that of nonlinear coefficient. Breakdown voltages (E_b) of doped samples decreased while the content of Pr_6O_{11} increased up to 0.05 mol%. But when the Pr_6O_{11} content exceeded 0.05 mol%, the E_b increased with it. The E_b values of all the doped samples were smaller than that of the pure WO_3.

The barrier voltages of doped WO_3 were 0.02–0.06 V, which were smaller than that of pure WO_3 (0.10–0.20 V), ZnO-based varistors (3–4 V) [16] and TiO_2-based varistors (0.1 V) [4]. So the WO_3-based varistors doped with Pr_6O_{11} were more suitable for low-voltage application.

Fig. 5 shows the dielectric constant vs. frequency of the WO_3-based samples. The dielectric constant of different samples at 1 kHz is shown in Table 1. Results showed that the dielectric constant of the samples doped with Pr_6O_{11} was larger than that of pure WO_3. While the content of the doped Pr_6O_{11} increased, the dielectric constant increased at first, reached the peak value of 8.53×10^4 with 0.05 mol% Pr_6O_{11}, and then decreased.

Fig. 6 shows the variation of resistivity vs. frequency. The resistivity decreased while the frequency increased, similar to the behavior of the dielectric constant. The properties measured in the low frequency region relied strongly on the character-

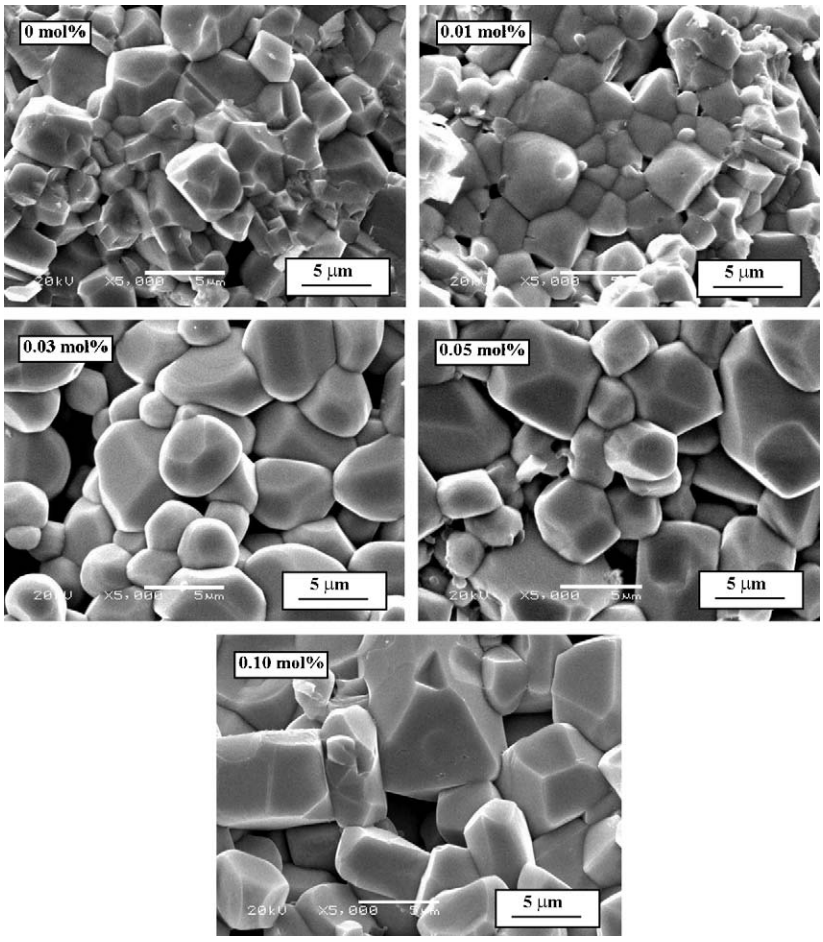

Fig. 2. SEM micrographs of WO_3 ceramics doped with different content of Pr_6O_{11}.

Table 1
Characteristics of WO_3 ceramics doped with Pr_6O_{11}.

Pr_6O_{11} (mol%)	E_b (V/mm)	α	v_b (V)	I_L (mA)	Φ_b	N_d ($\times 10^{25}/m^3$)	N_t ($\times 10^{17}/m^2$)	t (nm)	d (μm)	ε ($\times 10^4$) (f = 1 kHz)
0	19.6	2.5	0.10	0.55	0.276	1.12	2.04	18.2	5.1	0.11
0.01	16.1	2.9	0.06	0.51	0.294	2.33	3.48	14.9	3.6	3.12
0.03	8.5	3.8	0.05	0.35	0.315	3.36	4.12	12.3	5.7	7.69
0.05	3.7	3.2	0.02	0.44	0.302	2.83	2.91	10.2	6.2	8.53
0.10	5.1	2.3	0.04	0.62	0.263	1.95	3.23	16.6	8.7	4.89

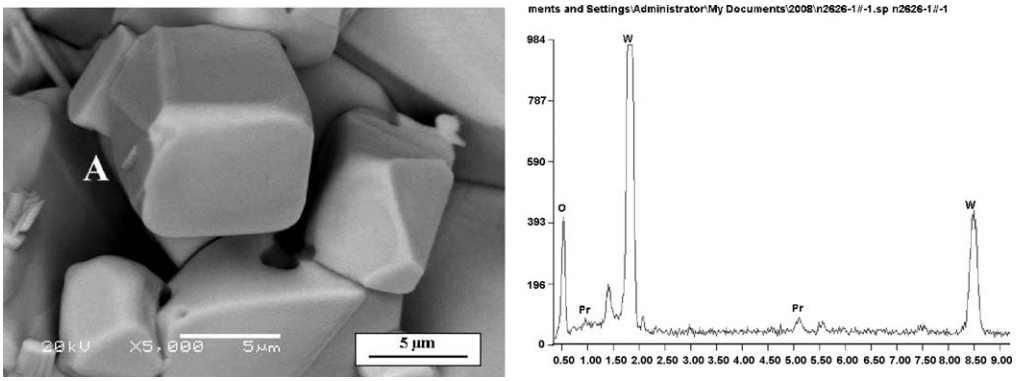

Fig. 3. SEM combined with EDX of WO_3–0.10 mol% Pr_6O_{11} sample.

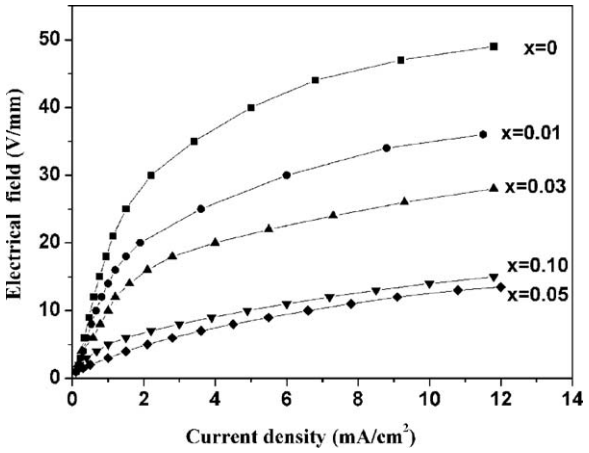

Fig. 4. The *I–V* characteristics of $(100-x)$ mol% $WO_3 + x$ mol% Pr_6O_{11} samples.

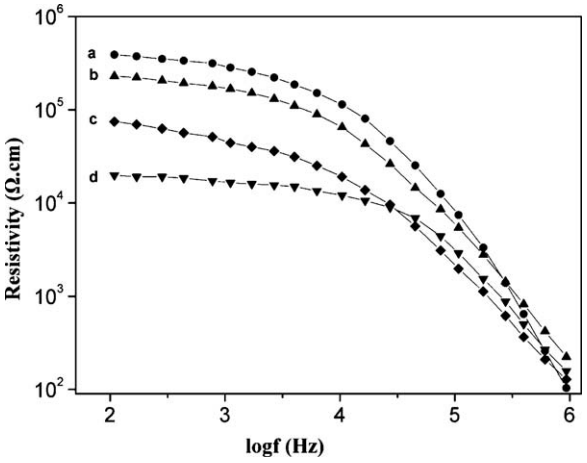

Fig. 6. The resistivity vs. frequency of samples with different Pr_6O_{11} content. (a) 0.03 mol%; (b) 0.05 mol%; (c) 0.01 mol%, (d) 0.10 mol%.

istics of the high resistivity and the width of the interfacial layer. And the properties measured in the high frequency region virtually reflected the properties of the low resistivity of grains, so the resistivity decreased while the frequency increased. The samples doped with 0.03 mol% Pr_6O_{11} exhibited the highest resistivity at low frequencies and a comparatively low resistivity at high frequencies.

The properties in the low frequency region resulted from high resistivity of grain-boundary layers, and the properties obtained in the high frequency region resulted from low resistivity of grains. The nonlinear coefficient (α) and the maximum nonlinear coefficient (α_{max}) had the following relation [17]:

$$\alpha = \frac{\alpha_{max}}{1+\xi} \tag{5}$$

where

$$\xi = \frac{R_g}{R_g + R_{gb}}(\alpha_{max} - 1) = \frac{1}{1 + (R_{gb}/R_g)}(\alpha_{max} - 1) \tag{6}$$

Where R_g was the grain resistance, R_{gb} was the grain-boundary resistance. It could be seen that the variation of α was in accordance with the variation of R_{gb}/R_g. Thus the sample doped with 0.03 mol% Pr_6O_{11} exhibited the largest nonlinear coefficient because it had the largest value of R_{gb}/R_g (Fig. 6).

The *C–V* characteristics of the samples are shown in Fig. 7 and Table 1. The Schottky interface voltage barrier height (Φ_b) was determined from the following expressions by thermionic emission mechanism in low field, Ohmic region.

$$J = AT^2 \exp\left[\frac{\beta E^{1/2} - \Phi_b}{kT}\right] \tag{7}$$

$$\ln J = \ln AT^2 + \frac{\beta E^{1/2} - \Phi_b}{kT} = \ln AT^2 - \frac{\Phi_b}{kT} + \frac{\beta}{kT}E^{1/2} \tag{8}$$

Where J was the forward current density, A was Richardson constant, E was the electric field, k was the Boltzmann's constant, and β was a constant related to the potential barrier width.

Plot of $\ln J$ vs. $E^{1/2}$ provided the straight line and the intercept of the line on vertical axis determined the Φ_b value, which could be obtained from the intersection of the extrapolated lines of the plot with the voltage axis. Compared the intercept value of vertical axis, the value of term AT^2 was

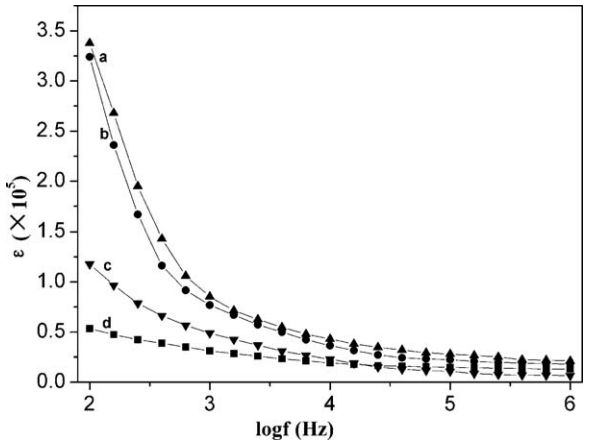

Fig. 5. The dielectric constant vs. frequency of samples with different Pr_6O_{11} content. (a) 0.05 mol%; (b) 0.03 mol%; (c) 0.10 mol%; (d) 0.01 mol%.

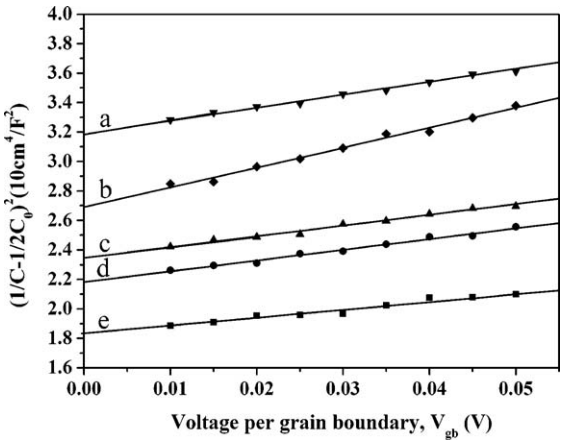

Fig. 7. The *C–V* characteristics of samples doped with different Pr_6O_{11} content. (a) 0.03 mol%; (b) 0.05 mol%; (c) 0 mol%; (d) 0.01 mol%; (e) 0.1 mol%.

very small and could be ignored. The relative magnitude of constant β could be derived from the slopes of the plots.

The doping of Pr_6O_{11} brought on the increase of the donor density (N_d) and the interface states density (N_t). The barrier height (Φ_b) increased with an increase of N_t. The depletion-layer width (t) calculated from N_d and N_t decreased from 18.2 nm to 8.9 nm. The highest grain-boundary barrier occurred in WO_3–0.03 mol% Pr_6O_{11}, which was consistent with the best nonlinear electrical properties for this composition.

The high dielectric constant of the ceramic arised from the fact that the resistivity of grains was much smaller than that of the grain-boundary layers, the entire voltage was sustained across narrow intergranular regions and the polarization was high [18]. The effective dielectric constant was given by Eq. (9) [19]:

$$\varepsilon = \varepsilon_b d/t \tag{9}$$

where ε_b was the internal dielectric constant of the barrier, d was the size of cubic grains and t was the mean thickness of the insulation barrier. The average grain size increased and t decreased with the increase of the Pr_6O_{11} content, so the d/t and ε increased. However, the superfluous Pr element segregated toward the grain-boundary interface and made the grain boundary wider. Therefore, the dielectric constant of samples decreased when the Pr_6O_{11} content exceeded 0.05 mol%.

The theory of defects in the crystal lattice [20] was introduced to explain the nonlinear electrical behavior of Pr_6O_{11}-doped WO_3 ceramics. During sintering, Pr_6O_{11} was decomposed to Pr_2O_3. Although Pr^{3+} had much larger radius (0.099 nm) than W^{6+} radius (0.060 nm), it remained possibility for a limited substitution, such as the following defect equation.

$$1/2Pr_2O_3 \xrightarrow{WO_3} Pr'''_W + 3/2V_O^{\bullet\bullet} + 3/2O_O \tag{10}$$

From Eq. (8), when a Pr^{3+} diffused into the WO_3 lattice and occupied W^{6+} site, three negative charges presented. Then 3/2 oxygen vacancy ($V_O^{\bullet\bullet}$) was created for the electric charge balance. While the doping content of Pr^{3+} increased, more oxygen vacancy created. They increased the electron-hopping probability and produced conductivity in grains. But Pr^{3+} behaved a limited substitution because it had a larger ionic radius and a lower valence than the W^{6+}. Most Pr^{3+} ions segregated at the WO_3 grain boundary to relieve elastic strain energy and thus increased grain boundary resistivity by acting as acceptors. They blocked the formation and transportation of electrons and defects. Owing to the above two reasons, the sample doped with 0.03 mol% Pr_6O_{11} obtained the most effective boundary barrier layer.

4. Conclusions

0.01 mol%–0.10 mol% Pr_6O_{11}-doped WO_3 ceramics were fabricated in this study. An optimal composition of WO_3–0.03 mol% Pr_6O_{11} was obtained with the breakdown voltage of 8.8 V/mm, the nonlinear coefficient of 3.8, and the dielectric constant of 7.69×10^4 at 1 kHz. The WO_3–0.03 mol% Pr_6O_{11} sample, in comparison with other samples, exhibited the highest resistivity at low frequencies, and a comparatively low resistivity at high frequencies. The good nonlinear properties of the WO_3–0.03 mol% Pr_6O_{11} originated from its high grain-boundary defect barriers.

Acknowledgments

Fund was supported by the State Key Laboratory of Advanced Technology for Materials Synthesis & Processing, Wuhan University of Technology, China (2008-ZD-1).

References

[1] T.K. Gupta, Application of zinc oxide varistors, J. Am. Ceram. Soc. 73 (7) (1990) 1817–1840.
[2] M. Houabes, R. Metz, Rare earth oxides effects on both the threshold voltage and energy absorption capability of ZnO varistors, Ceram. Int. 33 (2007) 1191–1197.
[3] M.F. Yan, W.W. Rhodes, Preparation and properties of TiO_2 varistors, Appl. Phys. Lett. 40 (1982) 536–537.
[4] W.Y. Wang, D.F. Zhang, T. Xu, Y.P. Xu, T. Zhou, B.Q. Hu, C.Y. Wang, L.S. Wu, X.L. Chen, Nonlinear electrical characteristics and dielectric properties of Ca, Ta-doped TiO_2 varistors, Appl. Phys. A 76 (2003) 71–75.
[5] V. Makarov, M. Trontelj, Novel varistor material based on tungsten oxide, J. Mater. Sci. Lett. 13 (1994) 937–939.
[6] A.G.S. Filho, J.G.N. Matias, N.L. Dias, V.N. Freire, Microstructural and electrical properties of sintered tungsten trioxide, J. Mater. Sci. 34 (1999) 1031–1035.
[7] X.S. Yang, Y. Wang, L. Dong, M. Chen, F. Zhang, L.Z. Qi, Effect of CeO_2 on the microstructure and electrical properties of WO_3 capacitor-varistor ceramics, Mater. Sci. Eng. B 110 (2004) 6–10.
[8] R.J.D. Tilley, Correlation between dielectric constant and defect structure of non-stoichiometric solids, Nature 269 (1977) 229–231.
[9] C.W. Nahm, The electrical properties and d.c. degradation characteristics of Dy_2O_3 doped Pr_6O_{11}-based ZnO varistors, J. Eur. Ceram. Soc. 21 (2001) 545–553.
[10] C.W. Nahm, Microstructure and electrical properties of Y_2O_3-doped ZnO–Pr_6O_{11}-based varistor ceramics, Mater. Lett. 57 (2003) 1317–1321.
[11] C.W. Nahm, Influence of La_2O_3 additives on microstructure and electrical properties of ZnO–Pr_6O_{11}-CoO-Cr_2O_3-La_2O_3-based varistors, Mater. Lett. 59 (2005) 2097–2100.
[12] Y. Wang, X.S. Yang, Z.L. Liu, K.L. Yao, Varistor effect of WO_3-based ceramics at high temperatures, Mater. Lett. 58 (2004) 1017–1019.
[13] X.S. Yang, Y. Wang, Y. Zhao, Effect of Dy_2O_3 and La_2O_3 on the microstructure and electrical properties of WO_3 ceramics, Mater. Chem. Phys. 98 (2006) 225–230.
[14] L.M. Lionel, H.R. Philipp, Zinc oxide varistors - A review, Ceram. Bull. 65 (4) (1986) 639–646.
[15] J.A. Park, Effect of Al_2O_3 on the electrical properties of ZnO–Pr_6O_{11}-based varistor ceramics, Phys. B 403 (2008) 639–643.
[16] M.H. Wang, K.A. Hu, B.Y. Zhao, N.F. Zhang, Electrical characteristics and stability of low voltage ZnO varistors doped with Al, Mater. Chem. Phys. 100 (2006) 142–146.
[17] F.M. Meng, Influence of sintering temperature on semi-conductivity and nonlinear electrical properties of TiO_2-based varistor ceramics, Mater. Sci. Eng. B 117 (2005) 77–80.
[18] C.P. Li, J.F. Wang, W.B. Su, H.C. Chen, Y.J. Wang, D.X. Zhuang, Effect of sinter temperature on the electrical properties of TiO_2-based capacitor-varistors, Mater. Lett. 57 (2003) 1400–1405.
[19] J.M. Wu, C.J. Chen, Dielectric properties of (Ba, Nb) doped TiO_2 ceramics: migration mechanism and roles of (Ba, Nb), J. Mater. Sci. 23 (1988) 4157–4164.
[20] T.K. Gupta, W.G. Carlson, A grain-boundary defect model for instability/stability of a ZnO varistor, J. Mater. Sci. 20 (1985) 3487–3500.